JACS
JOURNAL OF THE AMERICAN CHEMICAL SOCIETY

Article

pubs.acs.org/JACS

Deciphering the Biosynthetic Origin of L-*allo*-Isoleucine

Qinglian Li, Xiangjing Qin, Jing Liu, Chun Gui, Bo Wang, Jie Li, and Jianhua Ju*

CAS Key Laboratory of Tropical Marine Bio-resources and Ecology, Guangdong Key Laboratory of Marine Materia Medica, RNAM Center for Marine Microbiology, South China Sea Institute of Oceanology, Chinese Academy of Sciences, Guangzhou 510301, China

Supporting Information

ABSTRACT: The nonproteinogenic amino acid L-*allo*-isoleucine (L-*allo*-Ile) is featured in an assortment of life forms comprised of, but not limited to, bacteria, fungi, plants and mammalian systems including *Homo sapiens*. Despite its ubiquity and functional importance, the specific origins of this unique amino acid have eluded characterization. In this study, we describe the discovery and characterization of two enzyme pairs consisting of a pyridoxal 5′-phosphate (PLP)-linked aminotransferase and an unprecedented isomerase synergistically responsible for the biosynthesis of L-*allo*-Ile from L-isoleucine (L-Ile) in natural products. DsaD/DsaE from the desotamide biosynthetic pathway in *Streptomyces scopuliridis* SCSIO ZJ46, and MfnO/MfnH from the marformycin biosynthetic pathway in *Streptomyces drozdowiczii* SCSIO 10141 drive L-*allo*-Ile generation in each respective system. In vivo gene inactivations validated the importance of the DsaD/DsaE pair and MfnO/MfnH pair in L-*allo*-Ile unit biosynthesis. Inactivation of PLP-linked aminotransferases DsaD and MfnO led to significantly diminished desotamide and marformycin titers, respectively. Additionally, inactivation of the isomerase genes *dsaE* and *mfnH* completely abolished production of all L-*allo*-Ile-containing metabolites in both biosynthetic pathways. Notably, in vitro biochemical assays revealed that DsaD/DsaE and MfnO/MfnH each catalyze a bidirectional reaction between L-*allo*-Ile and L-Ile. Site-directed mutagenesis experiments revealed that the enzymatic reaction involves a PLP-linked ketimine intermediate and uses an arginine residue from the *C*-terminus of each isomerase to epimerize the amino acid *β*-position. Consequently, these data provide important new insight into the origins of L-*allo*-Ile in natural products with medicinal potential and illuminate new possibilities for biotool development.

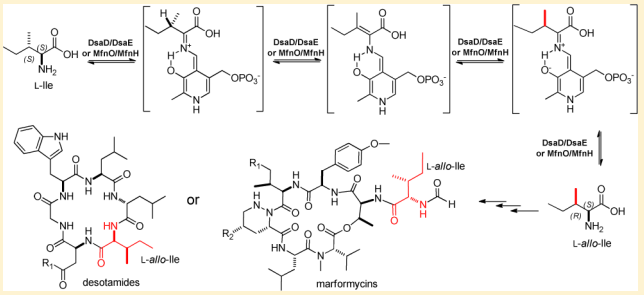

INTRODUCTION

Isoleucine contains two asymmetric centers and can therefore exist as any one of four possible stereoisomers, (2*S*,3*S*) L-isoleucine, (2*R*, 3*R*) D-isoleucine, (2*S*,3*R*) L-*allo*-isoleucine, and (2*R*,3*S*) D-*allo*-isoleucine (Figure 1A). The latter three nonproteinogenic amino acids have been found in nature. Of particular interest is L-*allo*-Ile which was originally reported in 1958.[1] The unique L-*allo*-Ile has been detected in plants,[2] found as a building block that is resistant to enzymatic digestion within cyclic peptide antibiotics [i.e., aureobasidin A,[3] cordyheptapeptides,[4] aspergillicin E[5] from fungi, and globomycin,[6] desotamides[7] and marformycins[8] from actinomycetes], and has been used as a precursor to synthesize the phytotoxin coronatine[9] from *Pseudomonas syringae* (Figure S1). Interestingly, L-*allo*-Ile is typically present in human plasma at barely detectable concentrations.[10−13] However, in people suffering from the inherited autosomal recessive disease maple syrup urine disease (MSUD) L-*allo*-Ile accumulates in plasma and urine, the result of a deficiency in mitochondrial branched-chain 2-ketoacid dehydrogenase activity.[13−17] Consequently, L-*allo*-Ile has been used as a pathognomonic marker (>5 μM in blood) in diagnosing MSUD patients.[13,17] Despite its structural similarity to L-Ile and ubiquity in various life kingdoms, the precise means of L-*allo*-Ile generation in living systems has long been a mystery; the biosynthetic enzymes and relevant mechanisms involved in L-*allo*-Ile production have eluded characterization.

We recently discovered two sets of cyclic peptide natural products from two deep South China Sea-derived *Streptomyces*. The desotamides[7] display antibacterial activities against pathogenic Gram-positive bacteria, and the marformycins[8] are bioactive against *Propionibacterium acnes* hinting at their potential for treating acne vulgaris (Figure 1B); most importantly, the rare L-*allo*-Ile moiety is represented in both classes of new natural products. We also have identified the gene clusters responsible for producing the desotamides in *Streptomyces scopuliridis* SCSIO ZJ46,[18] and the marformycins[19] from *Streptomyces drozdowiczii* SCSIO 10141; these efforts set the stage for deciphering the means by which L-*allo*-Ile is biosynthesized and subsequently used as a natural product building block. We report herein two enzyme pairs DsaD/DsaE and MfnO/MfnH that are functionally equivalent and drive the biosynthesis of L-*allo*-Ile during production of the desotamides and marformycins, respectively.

Received: November 7, 2015
Published: December 15, 2015

DOI: 10.1021/jacs.5b11380
J. Am. Chem. Soc. 2016, 138, 408−415

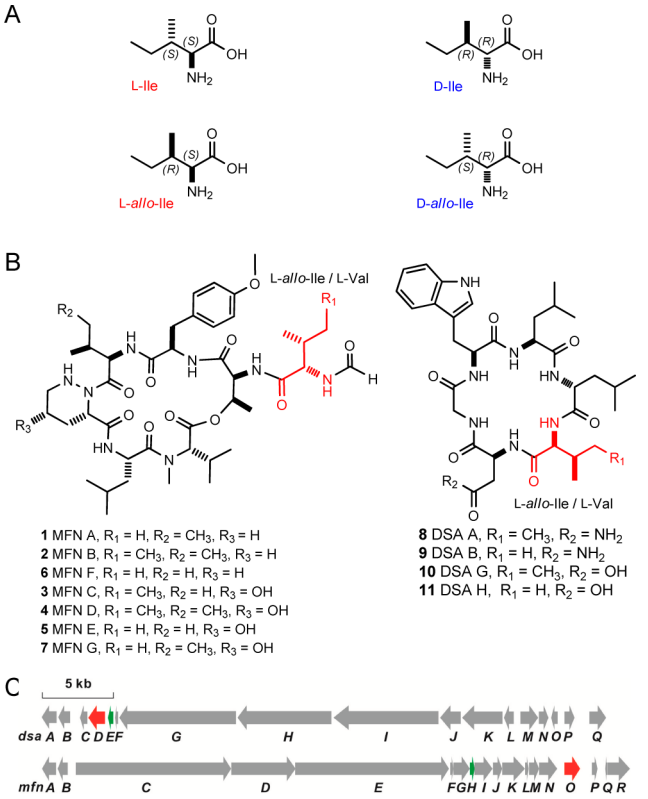

Figure 1. Structures of (A) the four stereoisomers of Ile and (B) marformycins and desotamides in which the L-*allo*-Ile moieties are shown in red. (C) The locations of the aminotransferase/isomerase pairs DsaD/DsaE and MfnO/MfnH in the DSA and MFN gene clusters, respectively. The aminotransferases DsaD/MfnO are shaded in red, and the isomerases DsaE/MfnH are shaded in green.

RESULTS AND DISCUSSION

Bioinformatics Analysis of DsaD/DsaE and MfnO/MfnH Enzyme Pairs in the Desotamides (DSA) and Marformycins (MFN) Biosynthetic Gene Clusters. Stereochemical comparisons between L-Ile and its diastereomer L-*allo*-Ile, revealed the only difference to be that of the β-carbon stereochemical configuration. The β-carbon stereochemistry was assigned as 3*S* for L-Ile and 3*R* for L-*allo*-Ile (Figure 1A). This realization inspired us to hypothesize that L-*allo*-Ile might originate from the natural amino acid L-Ile, and that the transformation might involve an L-Ile 2-deaminization process catalyzed by an aminotransferase followed by an isomerase-catalyzed 3-epimerization process. Bioinformatics analysis revealed that, *dsaD* in the DSA gene cluster, and *mfnO* in the MFN gene cluster, each encodes a typical aminotransferase. Sequence alignment revealed that these two proteins showed high sequence homology to the well-studied branched-chain aminotransferases (BCATs), and featured the conserved EXGXXNLFX$_n$LXTX$_n$LXGVXR signature motif found in all class-IV aminotransferases. DsaD and MfnO also both possess the conserved catalytic lysine residue covalently linked to pyridoxal 5′-phosphate (PLP) (Figure S2),[20−23] strongly suggesting their PLP-dependent aminotransferase activities. During efforts to identify isomerase candidates, BLASTP analyses failed to reveal clear candidates in either the DSA or MFN gene clusters. Subsequent structural homology searching was then performed using HHpred[24] revealing that the folding architecture of DsaE, a small protein (124 aa) coded for immediately upstream of the *dsaD* aminotransferase gene in the DSA gene cluster (Figure 1C), is shared with the nuclear transport factor 2 (NTF2) superfamily. The NTF2 superfamily contains thousands of functionally divergent proteins bearing low sequence homology to each other; members include the delta^5-3-ketosteroid isomerases (KSI) responsible for isomerizing delta^5-3-ketosteroid to delta^4-3-ketosteroid.[25] Accordingly, we envisioned that DsaE may be involved in the L-Ile β-carbon epimerization en route to L-*allo*-Ile. Notably, an orthologue of DsaE (identity: 42%; similarity: 56%), MfnH, was found in the MFN gene cluster. In contrast to *dsaE* which is located immediately upstream of *dsaD* within the DSA cluster, *mfnH* is located six open reading frames upstream of the aminotransferase *mfnO* gene within the MFN gene cluster (Figure 1C). The identification of aminotransferase/isomerase enzyme pairs in both the DSA and MFN gene clusters indicates a conserved biosynthetic logic in generating the L-*allo*-Ile precursor for these two sets of cyclic peptide natural products.

In Vivo Gene Inactivations of DsaD/DsaE and MfnO/MfnH and Resultant Metabolite Profiles in Desotamide and Marformycin Biosynthetic Pathways. To probe the exact roles of the DsaD/DsaE and MfnO/MfnH enzyme pairs in the biosynthesis of desotamides and marformycins, we inactivated *mfnO* and *mfnH* in *S. drozdowiczii* using established λ-RED-mediated PCR-targeting mutagenesis methods[26] (Figures S4 and S5). The Δ*mfnH* mutant failed to produce compounds **3** and **4** (MFNs C and D) both of which contain the L-*allo*-Ile moiety (Figure 1B and Figure 2A, trace iii). However, fermentations of the Δ*mfnH* mutant did afford compounds **5** and **7** (MFNs E and G) in which the L-*allo*-Ile moiety of the MFN scaffold was replaced by a corresponding L-Val moiety, as revealed by HPLC-UV, HPLC-MS and NMR data analyses. We noted that compound **7** (MFN G) has a

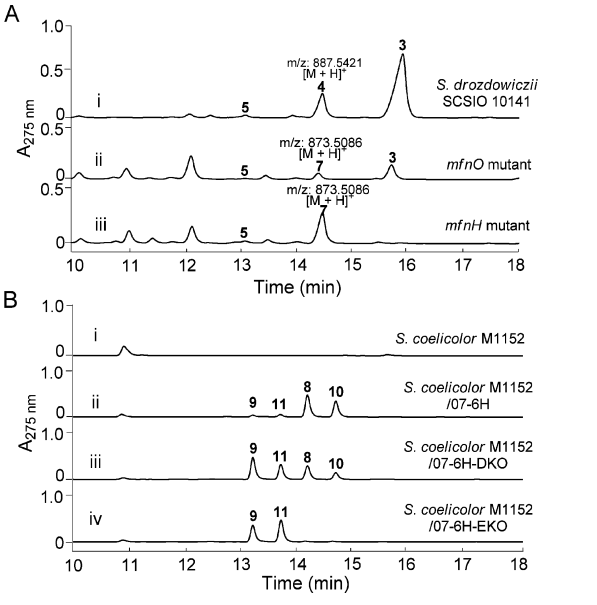

Figure 2. HPLC analyses of fermentation broths. (A) (i) marformycin wild-type producer *S. drozdowiczii* SCSIO 10141; (ii) Δ*mfnO* mutant strain; (iii) Δ*mfnH* mutant strain; (B) (i) negative control of the host strain *S. coelicolor* M1152; (ii) *S. coelicolor* M1152/07-6H harboring cosmid 07-6H with the intact DSA gene cluster; (iii) *S. coelicolor* M1152/07-6H-DKO harboring cosmid 07-6H with *dsaD* deleted; (iv) *S. coelicolor* M1152/07-6H-EKO harboring cosmid 07-6H with *dsaE* deleted.

DOI: 10.1021/jacs.5b11380
J. Am. Chem. Soc. 2016, 138, 408−415

retention time almost identical to that of **4** (MFN D) (Figure 2A, traces i–iii). Large-scale fermentation of the Δ*mfnH* mutant enabled isolation of quantities of **7** sufficient to support thorough structure elucidation and **7** was unambiguously assigned as a new compound containing a pendant L-Val moiety on the basis of comprehensive HRMS/MS, NMR data, and X-ray diffraction data analyses (Figures S8–S13). Fermentations of the Δ*mfnO* mutant afforded compounds **3** (MFN C), **5** (MFN E) and **7** (MFN G) (Figure 1B and Figure 2A, trace ii). The structures of **3** and **7** were confirmed following large scale fermentation, subsequent isolation, and HRMS/MS and NMR data comparisons with authentic samples. Although the Δ*mfnO* mutant retains the ability to produce **3** containing the L-*allo*-Ile moiety, its impaired biosynthetic capability, relative to that of the wild-type producer, may be explained by the presence of a compensatory aminotransferase elsewhere within the *S. drozdowiczii* SCSIO 10141 genome.

To explore the roles of *dsaD* and *dsaE*, each gene was in-frame deleted within the DSA cluster and heterologously expressed in the host strain *Streptomyces coelicolor* M1152 (Figures S6 and S7). *S. coelicolor* M1152 was selected as the host for these experiments because the natural DSA producer *S. scopuliridis* SCSIO ZJ46 is recalcitrant to genetic engineering.[18] The results of these heterologous expression experiments paralleled those obtained with *mfnO* and *mfnH* inactivations in *S. drozdowiczii*. The deletion of *dsaE* fully abolished production of L-*allo*-Ile-containing compounds **8** and **10** (DSAs A and G) (Figure 1B and Figure 2B, trace iv). However, the Δ*dsaE* mutant did produce **9** (DSA B) and **11** (DSA H); both **9** and **11** contain L-Val instead of L-*allo*-Ile. The deletion of *dsaD* correlated to production of the same four products **8**–**11**. However, the yields of **8** and **10** were significantly decreased and the yields of **9** and **11** were increased relative to those noted with the heterologously expressed full DSA pathway (Figure 1B and Figure 2B, traces ii and iii). This finding, as with those related to the MFN system, suggests that the loss of aminotransferase function by DsaD was partially compensated for by another enzyme within the *S. coelicolor* M1152 genome. The results of these in vivo gene inactivations clearly confirm the necessity of the DsaD/DsaE and MfnO/MfnH enzyme pairs in L-*allo*-Ile biosynthesis.

In Vitro Biochemical Characterization of DsaD/DsaE- and MfnO/MfnH-Catalyzed Interconversion between L-Ile and L-*allo*-Ile. To validate the in vitro biochemical activities of DsaD/DsaE and MfnO/MfnH enzyme pairs in L-*allo*-Ile biosynthesis, we overexpressed and purified DsaD, DsaE, MfnO and MfnH as soluble N-terminus His_6-tagged proteins from *E. coli* (Figure S14A). Both purified DsaD and MfnO proteins were yellow in color. The UV spectrum of DsaD exhibited an absorption band at 430 nm (Figure S14B), characteristic of PLP-dependent aminotransferases such as HspAT.[27] Denaturation of DsaD by boiling led to precipitation of the yellow protein and a colorless supernatant indicating the covalent nature of the PLP association with the catalytic lysine residue of DsaD; this association most likely involves a Schiff base linkage.

The activity of the DsaD/DsaE pair using L-Ile as a possible substrate was first explored. Initially, we incubated L-Ile with sole DsaD or DsaE in the presence of α-ketoglutarate (α-KG) and additional PLP in phosphate buffer (50 mM, pH 8.0). Under these conditions, L-Ile remained unchanged and none of the expected 3-methyl-2-oxyl-pentanoic acid product was observed upon chiral phase HPLC analysis of the reaction mixture (Figure S15A, traces iii and iv). DsaD, in isolation, failed to display classical aminotransferase activity. However, when such reactions contained both DsaD and DsaE, a new HPLC peak with a retention time corresponding to that of L-*allo*-Ile standard was observed (Figure S15A, trace v). We propose that the PLP copurified with DsaD might be sufficient for the DsaD/DsaE-catalyzed conversion of L-Ile to L-*allo*-Ile. To test this hypothesis and to ascertain the possible requirement of another cofactor, α-kG, for the DsaD/DsaE-catalyzed conversion of L-Ile to L-*allo*-Ile, exogenous PLP, α-kG and PLP/α-kG were removed from the reaction, respectively. The results of these efforts revealed that the intrinsic PLP copurified with DsaD is, in fact, sufficient to enable the L-Ile → L-*allo*-Ile conversion, and that α-kG is not required for the DsaD/DsaE-coupled reaction (Figure 3A and Figure S16A).

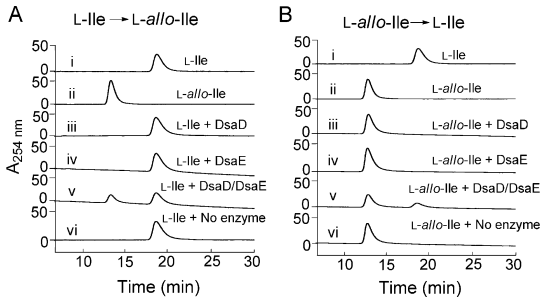

Figure 3. In vitro characterization of DsaD/DsaE. (A) Production of L-*allo*-Ile proceeds only upon coincubation of L-Ile with DsaD and DsaE (v). Enzyme assays with DsaD alone (iii), DsaE alone (iv), or control lacking DsaD/DsaE (vi) afforded only starting substrate L-Ile. (B) Production of L-Ile proceeds only upon coincubation of L-*allo*-Ile with DsaD and DsaE (v). Enzyme assays with DsaD alone (iii), DsaE alone (iv), or control lacking DsaD/DsaE (vi) afforded only starting substrate L-*allo*-Ile.

To further confirm the structure of the enzymatic product as L-*allo*-Ile, the enzymatic reaction containing L-Ile, DsaD and DsaE was performed on large-scale (10 mL); the product was purified by chiral-phase HPLC followed by heptanes-di(2-ethylhexyl)phosphonic acid (7:3) extraction, and finally, silica gel column chromatography (isocratic elution with butanol-acetic acid-H_2O, 4:1:5). The purified product, had the same molecular formula as that of L-*allo*-Ile as revealed by HRESIMS (Figure S17) and was found to yield ^{1}H NMR data identical to those previously reported for an authentic sample of L-*allo*-Ile (Figure S18).[3] Optical rotation and CD Cotton effect data for the newly generated species were also found to be identical to those of previously reported L-*allo*-Ile.[3] That generation of L-*allo*-Ile is contingent on the presence of both DsaD and DsaE suggests that these enzymes work synergistically to produce L-*allo*-Ile from Ile.

In the enzymatic assays, we found that the DsaD/DsaE-catalyzed conversion of L-Ile to L-*allo*-Ile proceeded in ≈60% yield no matter how long the reaction was allowed to proceed and regardless of moderate changes to reaction conditions such as pH and buffers. This indicated that the DsaD/DsaE-catalyzed reaction might be reversible. To test this idea, L-*allo*-Ile was coincubated with DsaD/DsaE under standard conditions, and a new peak with a retention time matching that of the L-Ile standard was observed (Figure 3B, trace v), demonstrating that, indeed, DsaD/DsaE catalyzed a reversible, bidirectional reaction. Furthermore, the production of L-Ile was

DOI: 10.1021/jacs.5b11380
J. Am. Chem. Soc. 2016, 138, 408–415

observed in the simultaneous presence of DsaD/DsaE, demonstrating that DsaD/DsaE act synergistically to generate L-Ile from L-*allo*-Ile.

We then determined the equilibrium constant for the DsaD/DsaE-catalyzed bidirectional reaction using equivalent concentrations of the enzyme pair. The resulting data show that the K_{eq} for the reaction with L-Ile as the substrate is 1.37 (Figure S19).

To validate the putative DsaD/DsaE substrate specificity, D-Ile and D-*allo*-Ile were evaluated as potential substrates. Co-incubation of D-Ile or D-*allo*-Ile with the DsaD/DsaE enzyme pair under standard assay conditions afforded no new species (Figure S20), indicating the stereospecificity of DsaD/DsaE-catalyzed chemistry and validating its relegation to L-Ile and L-*allo*-Ile interconversion.

The biochemical activity of the MfnO/MfnH enzyme pair was evaluated in a fashion similar to that applied to DsaD/DsaE. As anticipated, the MfnO/MfnH pair displayed a high degree of functional similarity with the DsaD/DsaE pair (Figures S15B and S21; Figure S16C and D). We additionally carried out experiments using the crossed enzyme pairs DsaD/MfnH and MfnO/DsaE. Importantly, both "crossed" pairs retained the ability to catalyze interconversion between L-Ile and L-*allo*-Ile suggesting cross compatibility between the relevant aminotransferase homologues and isomerase homologues (Figure S22). It is also notable that two highly homologous characterized BCATs from primary metabolism, EcBCAT from *E. coli* (NCBI gi number: 30749295)[21] and MsBCAT from *Mycobacterium smegmatis* MC^{2}155 (NCBI gi number: 399233140)[22] can also functionally substitute for DsaD (MfnO) (Figure S23); thus primary metabolism may, in some cases, play a compensatory role in L-*allo*-Ile generation.

Site-Directed Mutagenesis of DsaD/MfnO and DsaE/MfnH and a Proposed Catalytic Model for the Interconversion between L-Ile and L-*allo*-Ile. To probe the catalytic residues of aminotransferases DsaD/MfnO and the isomerases DsaE/MfnH, a series of site-directed mutagenesis experiments were performed. For the aminotransferases DsaD/MfnO, K198 in DsaD and K206 in MfnO were each converted to leucine. This mutation was inspired by the fact that residues homologous to K198 and K206 in DsaD/MfnO homologues identified by multiple sequence alignments are known to make Schiff bases with PLP and are responsible for elimination of the α-proton of the PLP-linked amino acid intermediate. The resultant K198L DsaD and K206L MfnO variants were overexpressed in *E. coli* BL21(DE3), purified (Figure S24A) and employed in enzymatic assays coupled with their respective isomerases DsaE or MfnH using L-Ile or L-*allo*-Ile as substrates. Not surprisingly, neither the DsaD nor the MfnO mutant displayed any activity (Figure 4A, traces iv and vi and Figure 4B, traces iv and vi). Moreover, supplementation of each reaction with additional PLP failed to return activity to either mutant enzyme pairing (Figure S25). These data highlight that K198 in DsaD and K206 in MfnO play essential, and likely similar, roles in their respective enzymatic transformations as reported for class-IV aminotransferases.

Although the folding architectures for isomerases DsaE and MfnH are shared with KSIs, these enzymes display low KSI sequence homology. As validated by biochemical and mutagenesis studies, as well as, X-ray crystallography, Tyr14, Asp99 and Asp38 represent the three catalytic residues in the KSI from *Comamonas testosteroni* (KSI_{Ct}); Tyr14 and Asp99 are involved in direct H-bonding interactions with the C3 oxyanion

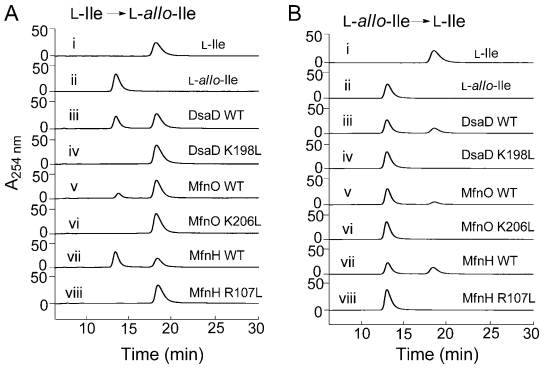

Figure 4. (A) Activity assays of DsaD/MfnO mutants (iv and vi) and the MfnH mutant (viii) using L-Ile as substrate by coupling with DsaE/MfnH or MfnO, respectively. (B) Activity assays of the DsaD/MfnO mutants (iv and vi) and the MfnH mutant (viii) using L-*allo*-Ile as substrate by coupling with their respective DsaE/MfnH or MfnO, respectively.

of the bound substrate and intermediate. The Asp38 is an essential catalytic residue that functions as a general base to intramolecularly transfer a proton from C4β to C6β.[25] Sequence alignment revealed that, within MfnH, DsaE, and their homologues, in the same corresponding positions, Tyr14 and Asp99 of KSI_{Ct} appear to be conserved (Tyr10 and Asp95 as seen in MfnH). However, the most important catalytic Asp38 of KSI_{Ct} is replaced with an arginine (Arg34) in MfnH (Figure S3A), indicating that MfnH and DsaE might utilize a mechanism different from that of traditional KSIs to carry out L-Ile β-carbon epimerization.

To interrogate the catalytic residues of isomerases MfnH/DsaE, we aligned the two proteins with 10 closely related proteins with undefined functions on the basis of BLAST results from the NCBI database. The purpose of this alignment was to unveil potentially conserved amino acid residues (Figure S3B) across the 12 enzymes. In addition to the three residues Tyr10, Arg34, Asp95 (corresponding to the three catalytic residues Tyr14, Asp38 and Asp99 of KSI_{Ct}), another 10 polar amino acids Tyr11, Asp15, Phe26, Tyr32, Phe49, Tyr50, Arg54, His61, Phe79, Arg107 of MfnH, conserved in MfnH/DsaE and their homologues, were mutated to nonpolar or nonactive residues. Consequently, 13 MfnH variants were constructed and overexpressed in *E. coli* BL21(DE3). Eight of the 13 MfnH variants were readily purified to homogeneity as soluble proteins (Figure S24B); and two MfnH variants (F26A and F79A) were overexpressed and partially purified due to the low yield of the specific proteins in soluble form (Figure S24C); the remaining three MfnH variants (D15L, H61F and D95L) were overexpressed but resisted even partial purification. Additionally, the D22, H68 and D102 residues of DsaE, corresponding to D15, H61 and D95 of MfnH, were also mutated and the resulting mutant enzymes were partially purified (Figure S24D). The purified or partially purified mutant proteins were employed in enzymatic assays involving MfnO or DsaD and using L-Ile or L-*allo*-Ile as substrates. HPLC analyses of the reaction mixtures revealed that the R107L MfnH mutant was completely devoid of enzymatic activity (Figure 4A, trace viii and Figure 4B, trace viii). The R34L MfnH mutant, together with the D22L, H68F and D102L DsaE mutants, displayed sharply reduced enzymatic activity; relative to wild-type MfnH/DsaE these mutants were only 8% active (Figure S26C and D). The remaining eight mutations introduced to MfnH exerted no

DOI: 10.1021/jacs.5b11380
J. Am. Chem. Soc. 2016, 138, 408−415

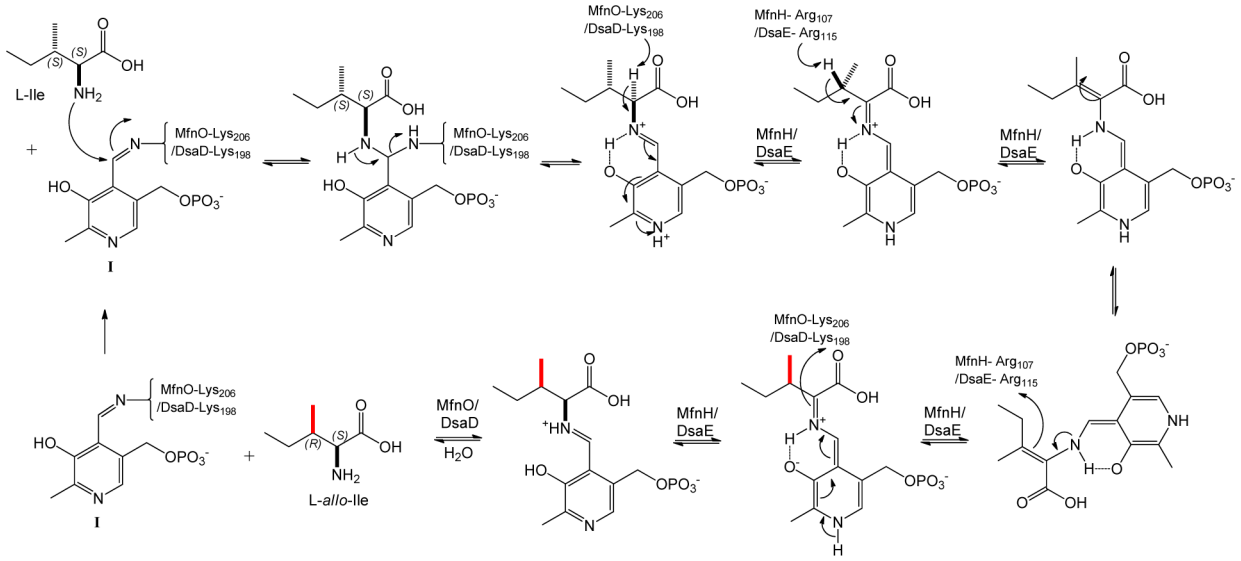

Figure 5. Proposed mechanism of DsaD/DsaE or MfnO/MfnH.

apparent effects upon enzymatic activity (Figure S26A and B). Consequently, it was realized that R107 in MfnH, and the corresponding R115 in DsaE, represent essential active site residues for this family of isomerases. Importantly, the active sites of MfnH/DsaE, identified on the basis of these mutagenesis studies, differ from those of KSI_{Ct}, thereby demonstrating that MfnH/DsaE represent a new family of isomerase.

On the basis of these site-directed mutagenesis experiments, we envision a rational model for the two enzyme-catalyzed bidirectional reaction between L-Ile and L-*allo*-Ile (Figure 5). The K206 of MfnO (or K198 of DsaD) initially forms a PLP-linked Schiff base (Figure 5, PLP-E complex **I**) followed by enzyme displacement (with retention of close noncovalent associations between the enzyme and newly formed substrate-PLP complex) upon presentation with substrate L-Ile (or L-*allo*-Ile). The new PLP-substrate complex, like the preceding PLP species, is a Schiff base. Second, the terminal amino group of newly liberated K206 then removes the C_α-proton of the PLP-substrate complex yielding a quinonoid intermediate. The third step in the envisioned pathway invokes the use of Rl07 in MfnH (or R115 in DsaE) to deprotonate the C_β-proton; this is enabled, in part, by acidification of the C_β proton resulting from earlier C_α deprotonation. Subsequent reprotonation of the transient enamine ($C_{\alpha\beta}$ olefin) at C_β on the face opposite that involved in C_β deprotonation installs the inverted C_β stereochemistry. Penultimately, the ammonium salt of Lys206 within MfnO (or K198 of DsaD) can reprotonate the C_α-position on the same stereochemical face as had been used for C_β reprotonation by R107 (MfnO) or R115 (DsaD) affording the C_β epimerized product L-*allo*-Ile. Finally, product release is envisioned to occur by PLP scission and reassociation with MfnO or DsaD through standard Schiff base formation with either K206 (MfnO) or K198 (DsaD), respectively (regenerating **I**). Notably, the mechanism envisioned here is clearly reversible as is reflected by Figure 5 as well as our observations that L-Ile serves not only as a substrate but also a product of Mfn and Dsa enzyme pair chemistries.

Phylogenetic Analysis of DsaE/MfnH Unveils a Family of Related Proteins Potentially Functioning as Isomerases Biosynthesizing L-*allo*-Ile. Phylogenetic analyses of DsaE and MfnH with related proteins in the Genbank database revealed that they belong to a family of proteins with unknown functions represented across two domains, the Bacteria and Archaea (Figure S27). Homologous proteins from the Bacteria domain include proteins from actinomycetes such as *Streptomyces*, *Nocardiopsis*, and *Salinispora* that have a demonstrated record of producing bioactive natural products, but also contain proteins from actinobacteria such as *Actinokineospora*, *Dermacoccus*, and *Actinoplanes*, as well as *Proteobacteria* such as *Burkholderia* and *Oceanospirillaceae* (*Osedax* symbiont), *Deinococcus*, and members of *Clostridiales* whose secondary metabolites have only been marginally investigated. It is noteworthy that DsaE and MfnH also have a large number of homologous proteins from Archaea including *Halobacteriaceae* and *Thermoplasmatales*, secondary metabolites from which have been largely unexplored. Thus, DsaD/DsaE or MfnO/MfnH pairs might serve as effective genetic markers enabling genome mining-based identification of natural products containing the L-*allo*-Ile moiety.

CONCLUSION

L-*allo*-Ile is a crucial building block for bioactive natural products from various microorganisms and exists in the free form within assorted life forms including *Homo sapiens*; its functional role in many such scenarios remains the topic of speculation. To decipher and understand the origin of L-*allo*-Ile we studied the biosynthetic machineries for two groups of anti-infective natural products, the desotamides and marformycins; representatives of both natural product classes contain the unique L-*allo*-Ile. Bioinformatics analyses of both biosynthetic pathways revealed two conserved enzyme pairs DsaD/DsaE and MfnO/MfnH as candidates involved in generating the L-*allo*-Ile unit found in the desotamides and marformycins. In vivo gene inactivation trials coupled with metabolomics and in vitro biochemical characterizations revealed that the DsaD/DsaE and MfnO/MfnH enzyme pairs drive bidirectional interconversion of L-Ile and L-*allo*-Ile. Site-directed mutagenesis experiments revealed that this interconversion proceeds through a PLP-linked L-Ile (or L-*allo*-Ile) intermediate; a lysine residue of aminotransferases DsaD or MfnO removes the α-proton, and an arginine residue from the *C*-terminus of

DOI: 10.1021/jacs.5b11380
J. Am. Chem. Soc. 2016, 138, 408−415

isomerases DsaE or MfnH, respectively deprotonate and subsequently reprotonate the L-*allo*-Ile β-position. Following this epimerization by either the DsaE or MfnH arginine, the lysine residue of aminotransferase DsaD or MfnO previously used for C_α-deprotonation, stereospecifically reprotonates the α-position, leading to retention of the original C_α stereochemistry. Phylogenetic analyses validate DsaE and MfnH as representatives of a new isomerase family within Bacteria and Archaea domains whose exact functions have not yet been assigned. In addition to shedding light on the role of this isomerase family, our work here explains the mysterious biosynthesis of L-*allo*-Ile in actinomyces. These findings lay the foundation for further studies into the origins of L-*allo*-Ile in assorted living systems. The findings disclosed herein also point the way to discovery (likely through genome mining) and development of other L-*allo*-Ile containing compounds with possible therapeutic and/or biomedical applications. The well-established elevated L-*allo*-Ile levels in humans suffering from maple syrup urine disease, in particular, gives cause for significant excitement in the biomedical and diagnostics arena.

EXPERIMENTAL SECTION

Bacterial strains, Plasmids, Culture Conditions, and Reagents. The marformycin producer *Streptomyces drozdowiczii* SCSIO 10141[19] and desotamide producer *Streptomyces scopuliridis* SCSIO ZJ46[18] have been previously described. *S. coeliecolor* M1152 was used as the host strain for heterologous expression of the desotamide gene cluster and has also been described. *Escherichia coli* DH5α was used as the host for cloning purposes. *E. coli* ET12567/pUZ8002 was used to transfer DNA into the *Streptomyces* from *E. coli* by conjugation. *E. coli* BW25113/pIJ790 was used as the host for Red/ET-mediated recombination for inactivation of *dsaD*, *dsaE*, *mfnO* and *mfnH*. All *E. coli* strains were grown in Luria−Bertani medium at 37 or 30 °C. When used, antibiotics were introduced at the following concentrations: apramycin (Apr, 50 μg/mL), kanamycin (Kan, 50 μg/mL), ampicillin (Amp, 100 μg/mL), spectinomycin (Spec, 50 μg/mL), chloramphenicol (Chl, 25 μg/mL), and trimethoprim (TMP, 50 μg/mL). L-*allo*-Ile and Ile were purchased from Sigma-Aldrich Co. LLC. Other chemicals and solvents were purchased from standard commercial sources.

NMR data were acquired using an Avance 500 MHz spectrometer instrument (Bruker). High resolution mass spectra data were determined with a Maxis quadrupole-time-of-flight mass spectrometer (Bruker). Optical rotation was obtained with an MCP-500 polarimeter (Anton Paar). The UV spectrum was recorded with a UV-2600 spectrometer (Shimadzu). CD spectra were obtained with a Chirascan circular dichroism spectrometer at 25 °C. The crystal structure data for compound **7** were recorded with an Oxford Xcalibur Onyx Nova single-crystal diffractometer with Cu Kα radiation (λ = 1.5418 Å); the structure was solved by direct methods (SHELXS-97) and refined using full-matrix least-squares difference Fourier techniques.

Gene Inactivation of *mfnO*, *mfnH*, *dsaD*, and *dsaE*. The genes *mfnO* and *mfnH* were inactivated in wild-type strain *S. drozdowiczii* SCSIO 10141 using λ-RED mediated PCR-targeting technology. First, a 1425 bp spectinomycin resistance gene as a PCR template was obtained by digestion of plasmid pIJ778 by *Hin*dIII/*Eco*RI. Then, each of the spectinomycin resistance gene cassettes (*oriT-aadA*) was amplified by PCR using the obtained template with designed primers listed in Table S1. Subsequently, the PCR-targeting and conjugation processes were carried out as described previously.[19] Double-crossover mutant strains Δ*mfnO* and Δ*mfnH* possessing the kanamycin^S and spectinomycin^R phenotypes were confirmed by PCR using primers listed in Table S1.

For in-frame deletion of *dsaD* and *dsaE* within the desotamide gene cluster from *S. scopuliridis* SCSIO ZJ46, the SuperCos 1 vector based cosmid 07-6H harboring the intact desotamide gene cluster was used. Each of the apramycin resistance gene cassettes (*aac(3)IV-oriT*) was amplified by PCR using the obtained template with designed primers (with *Spe*I restriction site between the 19 or 20 nt matching the right or left end of the disruption cassette and the 39 nt homologous to the gene to be inactivated) listed in Table S1. Each apramycin resistance cassette was introduced into *E. coli* BW25113/pIJ790/07-6H (harboring the intact desotamide gene cluster) by electroporation to disrupt the homologous gene region in the cosmid 07-6H. The mutated cosmids 07-6H-DKO and 07-6H-EKO were digested with *Spe*I and then self-ligated. The resulting cosmids 07-6H-DKO-IF and 07-6H-EKO-IF lost the (*aac(3)IV-oriT*) cassette and were screened with primers listed in Table S1. For heterologous expression of cosmids 07-6H-DKO-IF and 07-6H-EKO-IF in *S. coelicolor* M1152, they were modified by replacing each kanamycin resistance gene within the SuperCos 1 vector with a pSET152AB-derived fragment. The pSET152AB vector constructed in our laboratory using RED recombination approaches contains an apramycin resistance gene and elements for conjugation and site specific recombination (*oriT*, integrase gene and *int*ψ*C31* site).[28] The resulting cosmids, designated 07-6H-DKO-AB and 07-6H-EKO-AB were transferred into *S. coelicolor* M1152 by conjugation and stable integration into their chromosomes via *attB/attp*-site-specific recombination, to yield *S. coelicolor* M1152/07-6H-DKO, *S. coelicolor* M1152/07-6H-EKO strains, respectively.

Metabolite Analyses of Wild-Type and Mutant Strains. The fermentations and subsequent HPLC analyses of the fermentation broths of wild-type *S. drozdowiczii* SCSIO 10141 and its mutant strains were carried out as described previously.[19] Fermentations and subsequent HPLC analyses of the fermentation broths of the recombinant heterologous DSA gene cluster (intact gene cluster or the cluster with *dsaD* or *dsaE* deleted) expression strains were also carried out as described previously.[18]

Isolation and Structural Elucidation of Compounds 3, 5 and 7. The Δ*mfnH* mutant was fermented using 1 L Erlenmeyer flasks each containing 250 mL production medium as described previously.[19] After fermentation, the culture (8 L) was centrifuged to yield supernatant and a mycelial cake. The supernatant was extracted three times with equal volumes of butanone. The mycelial cake was extracted three times with acetone. The two extracts were combined and the organic solvent was removed under reduced pressure to afford 10.2 g of residue which was further subjected to normal phase silica gel column chromatography (100−200 mesh). The residue was eluted using gradient elution with $CHCl_3$ and CH_3OH mixtures (100:0, 98:2, 96:4, 94:6, 96:4, 90:10, v/v, each solvent combination used was 100 mL in volume) to afford six fractions (Fr.1−Fr.6). Fr.3 was further subjected to normal phase silica gel column chromatography (100−200 mesh), and eluted with $CHCl_3$ and CH_3OH mixtures (100:0, 98:2, 96:4, 94:6, 96:4, 90:10, v/v, each solvent combination in 50 mL volume) affording six subfractions (Fr.3−1−Fr.3−6). Then Fr.3−3 was separated by semipreparative HPLC (YMC-Pack ODS-A column, 250 × 10 mm, 5 μm) eluted with a linear gradient from 40% to 100% B (solvent A: H_2O, solvent B: CH_3CN) over 30 min and using UV detection at 225 and 275 nm to give compounds **5** (6.5 mg) and **7** (8.0 mg).

The Δ*mfnO* mutant was similarly fermented (8 L) and processed. The butanone extract of the supernatant and acetone extract of the mycelia were combined and subjected to normal phase silica gel column chromatography (100−200 mesh), and eluted with $CHCl_3$ and CH_3OH mixtures (100:0, 98:2, 96:4, 94:6, 96:4, 90:10, 80:20, 50:50, v/v, 100 mL for each solvent combination used) to afford eight fractions (Fr.1−Fr.8). Fr.3 was repeatedly subjected to normal phase silica gel column chromatography (100−200 mesh), and eluted with $CHCl_3$ and CH_3OH mixtures (100:0, 98:2, 96:4, 94:6, 96:4, 90:10, v/v, each solvent combination in 50 mL volume) affording six fractions (Fr.3−1−Fr.3−6). Fr.3−2 and Fr.3−3 were combined and further isolated by semipreparative HPLC (YMC-Pack ODS-A column, 250 × 10 mm, 5 μm) eluted with a linear gradient from 40% to 100% B (A: H_2O, B: CH_3CN) over 30 min and with UV detection at 225 and 275 nm to yield compounds **3** (5.3 mg), **5** (8.0 mg) and **7** (14.4 mg). Compound **7**, white powder; $[\alpha]_D^{25}$ −72°, (*c* 0.98, MeOH); HR-ESI-MS (*m*/*z*): 873.5086 $[M + H]^+$ (calc. for $C_{43}H_{69}N_8O_{11}$, 873.5080).

DOI: 10.1021/jacs.5b11380
J. Am. Chem. Soc. 2016, 138, 408−415

Cloning, Expression, and Purification of DsaD, DsaE, MfnO, MfnH, EcBCAT, MsBCAT, DsaD Mutant, MfnO Mutant, MfnH Mutants and DsaE Mutants. The genes for *dsaD*, *dsaE*, *mfnO*, *mfnH* were PCR amplified from genomic DNA of *S. scopuliridis* SCSIO ZJ46 and *S. drozdowiczii* SCSIO 10141, respectively. And the genes for EcBCAT and MsBCAT were PCR amplified from genomic DNA of *E. coli* DH5α and *Mycobacterium smegmatis* MC^{2}155, respectively. The gel-purified PCR products were digested with *Nde*I/*Eco*RI (for *dsaD*, *dsaE*, *mfnO* and *mfnH*) or *Nhe*I/*Eco*RI (for EcBCAT and MsBCAT) and then ligated into the same sites of pET28a (+) to yield the expression plasmids pET28a/dsaD, pET28a/dsaE, pET28a/mfnO, pET28a/mfnH, pET28a/EcBCAT and pET28a/MsBCAT; these were confirmed for correctness by DNA sequencing. The resulting expression plasmids were each transformed into *E. coli* BL21 (DE3) for protein expression. Expression and purification of all proteins was carried out following the general procedure previously described.[29] The fractions containing proteins of interest were pooled, desalted by passage through a PD-10 column (GE Healthcare, USA), and concentrated by ultrafiltration (Millipore membrane, 3 kDa cutoff). The purified proteins were finally stored in 10% glycerol, 50 mM sodium phosphate buffer, pH 8.0 for further experiments at −80 °C. Protein concentrations were determined by Bradford assays using bovine serum albumin as a standard.

The site-directed mutations of DsaD, MfnO, MfnH and DsaE were performed following the Fast Mutagenesis System (Transgen, Beijing, China) manual protocol. The expression and purification of mutant proteins was carried out using the same procedures described above. All primers used here are listed in Table S1.

In Vitro Enzymatic Assays.

(a) The enzymatic assays investigating stand-alone DsaD, DsaE, MfnO, MfnH activities and DsaD/DsaE or MfnO/MfnH-catalyzed coupled reactions in the presence of α-ketoglutarate (α-KG) and additional exogenous PLP were performed in a volume of 100 μL, at 30 °C for a period of 4 h. Reaction mixtures contained 5 μM enzyme, 1 mM substrate L-Ile or L-*allo*-Ile, 1 mM α-KG, and 0.1 mM PLP in 50 mM sodium phosphate buffer (pH 8.0).

(b) Assays for determination of the necessity of the possible cofactor α-KG and additional cofactor PLP for the DsaD/DsaE or MfnO/MfnH-catalyzed interconversion between L-Ile and L-*allo*-Ile, each cofactor was omitted from the reaction mixture containing 5 μM aminotransferase DsaD (or MfnO), 5 μM isomerase DsaE (or MfnH), 1 mM α-KG, 0.1 mM PLP and 50 mM sodium phosphate buffer (pH 8.0) at a time.

(c) The enzymatic assays assessing stand-alone DsaD, DsaE, MfnO, MfnH activities or the DsaD/DsaE, MfnO/MfnH, DsaD/MfnH and MfnO/DsaE-catalyzed coupled reactions in the absence of α-KG and additional exogenous PLP were performed in a volume of 100 μL, 30 °C for 4 h. Each reaction mixture contained 5 μM enzyme/s, and 1 mM substrate L-Ile or L-*allo*-Ile in 50 mM sodium phosphate buffer (pH 8.0). These reaction conditions were used as the standard assay conditions for DsaD/DsaE activity assays.

(d) Assays used to investigate substrate specificities for DsaD/DsaE or MfnO/MfnH were performed in a volume of 100 μL, 30 °C for 4 h. Each reaction mixture contained 5 μM aminotransferase DsaD or MfnO, 5 μM isomerase DsaE or MfnH, and 1 mM substrate D-Ile or D-*allo*-Ile in 50 mM sodium phosphate buffer (pH 8.0).

(e) Assays to investigate the activity of aminotransferase DsaD/MfnO mutants as coupled with their respective isomerases DsaE or MfnH were performed in a volume of 100 μL, 30 °C for 4 h. Each reaction mixture contained 5 μM DsaD or MfnO mutant, 5 μM isomerase DsaE or MfnH, and 1 mM substrate L-Ile or L-*allo*-Ile in 50 mM sodium phosphate buffer (pH 8.0).

(f) The enzymatic assays to evaluate activities of MfnH/DsaE mutants as coupled with their respective aminotransferase pair MfnO or DsaD were performed in a volume of 100 μL, 30 °C for 4 h. The reaction mixtures contained 5 μM MfnH or DsaE mutant, 5 μM aminotransferase MfnO or DsaD, 0.1 mM PLP and 1 mM substrate L-Ile or L-*allo*-Ile in 50 mM sodium phosphate buffer (pH 8.0).

(g) Assays to investigate the activity of EcBCAT and MsBCAT coupled with the isomerases DsaE or MfnH were performed in a volume of 100 μL, 30 °C for 4 h. The reaction mixtures contained 5 μM MsBCAT or EcBCAT, 5 μM isomerases DsaE or MfnH, and 1 mM substrate L-Ile or L-*allo*-Ile in 50 mM sodium phosphate buffer (pH 8.0).

All reactions were quenched by addition of 200 μL MeOH. After incubation for 20 min at room temperature, the precipitated proteins were removed by centrifugation (12 000*g* for 20 min at room temperature). Supernatants were dried in vacuo and the resulting residues dissolved in 40 μL 2 mM $CuSO_4$ aqueous solution and 25 μL of each was subjected to chiral-phase HPLC analyses performed on an Agilent Technologies 1260 Infinity system using an MCI GEL CRS10W column (Mitsubishi, 50 × 4.6 mm, 3 μm) eluted with 2 mM $CuSO_4$ aqueous solution over the course of 30 min at a flow rate of 1 mL/min and with UV detection at 254 nm.

Enzymatic Synthesis and Isolation of L-*allo*-Ile. For production and isolation of L-*allo*-Ile, a large-scale enzymatic reaction was performed in 10 mL sodium phosphate buffer (50 mM, pH 8.0) containing 2 mM L-Ile, 20 μM DsaD, 20 μM DsaE at 30 °C for 4 h. The reaction was quenched by addition of 20 mL MeOH to precipitate the proteins and the solvent was removed in vacuo. The resulting residues were dissolved in 2 mM $CuSO_4$ aqueous solution, and purified by chiral-phase HPLC using an MCI GEL CRS10W column (Mitsubishi, 50 × 4.6 mm, 3 μm) eluted with 2 mM $CuSO_4$ aqueous solution at a flow rate of 1 mL/min and employing UV detection at 254 nm. The fraction with a retention time of 13 min was pooled, ethylene diamine tetraacetic acid (EDTA) was added to a final concentration of 2 mM and the pH of the subsequent mixture adjusted to 4.0. The mixture was extracted using heptane-di(2-ethylhexyl)-phosphonic acid (7:3) twice, and the combined organic layer was further extracted by equal volumes of 5% HCl solution twice. The combined aqueous layer was evaporated to dryness, and finally purified by silica gel column chromatography (isocratic elution with the upper layer of butanol-acetic acid-H_2O (4:1:5)), yielding pure L-*allo*-Ile as a white solid.

Enzymatically Produced L-allo-Ile. HR-ESI-MS $[M + H]^+$ = 132.1038 (calc. for $C_6H_{14}NO_2$, 132.1019); ^{1}H NMR (500 MHz, D_2O), δ 0.86 (3H, t, J = 7.5 Hz), 0.83 (3H, d, J = 7.0 Hz), 1.19−1.40 (2H, m), 1.96 (1H, m), 3.62 (1H, m). $[\alpha]_D^{25}$ + 23.4° (*c* 0.0575, aq HCl, pH 2.5). CD $[\theta]_{202}$ + 165.7° (*c* 0.0575, aq HCl, pH 2.5).

L-allo-Ile Standard. ^{1}H NMR (500 MHz, D_2O), δ 0.86 (3H, t, J = 8.0 Hz), 0.84 (3H, d, J = 7.0 Hz), 1.20−1.40 (2H, m), 1.98 (1H, m), 3.64 (1H, m). $[\alpha]_D^{25}$ + 23.2° (*c* 0.1, aq HCl, pH 2.5). CD $[\theta]_{202}$ + 333.3° (*c* 0.1, aq HCl, pH 2.5).

Equilibrium Constant of DsaD/DsaE. Assays to establish equilibrium constants were performed in 50 μL sodium phosphate buffer (50 mM, pH 8.0) containing 2.5 μM DsaD, 2.5 μM DsaE, 0.1 mM PLP and 5 mM of substrate L-Ile or L-*allo*-Ile at 30 °C in triplicate. Each reaction was stopped by addition of 150 μL of methanol at times of 2.5, 5, 10, 15, 25, 30, 40, 60, 120, 180, and 240 min. Subsequent treatment of reaction mixtures and HPLC analyses were conducted using the same methods applied to the standard DsaD/DsaE activity assays. The final concentrations of substrates and products were calculated on the basis of fraction peak integrals. The K_{eq} was calculated using the equation K_{eq} = ([product]/[substrate]) when the reaction achieved equilibrium.

■ ASSOCIATED CONTENT

Supporting Information

The Supporting Information is available free of charge on the ACS Publications website at DOI: 10.1021/jacs.5b11380.

Supporting figures and tables. (PDF)

Crystal data. (CIF)

DOI: 10.1021/jacs.5b11380
J. Am. Chem. Soc. 2016, 138, 408−415

AUTHOR INFORMATION

Corresponding Author

*jju@scsio.ac.cn

Notes

The authors declare no competing financial interest.

ACKNOWLEDGMENTS

This study was supported, in part, by the National Natural Science Foundation of China (31400072, 81425022, 41306146), the National High Technology Research and Development Program of China (2012AA092104), the Programs of Chinese Academy of Sciences (XDA11030403, KGZD-EW-606), and a special financial fund for innovative developments of the Marine Economic Demonstration Project (GD2012-D01-001). Additionally, we thank the analytical facility center (Ms. Aijun Sun, Dr. Zhihui Xiao and Mr. Chuanrong Li) of the South China Sea Institute of Oceanology for recording NMR and MS data.

REFERENCES

(1) Van Dam-Bakker, A. W. *Nature* **1958**, *181*, 116.
(2) Ali, H. S.; Alhaj, O. A.; Al-Khalifa, A. S.; Brückner, H. *Amino Acids* **2014**, *46*, 2241.
(3) Ikai, K.; Takesako, K.; Shiomi, K.; Moriguchi, M.; Umeda, Y.; Yamamoto, J.; Kato, I.; Naganawa, H. *J. Antibiot.* **1991**, *44*, 925.
(4) Chen, Z.; Song, Y.; Chen, Y.; Huang, H.; Zhang, W.; Ju, J. *J. Nat. Prod.* **2012**, *75*, 1215.
(5) Capon, R. J.; Skene, C.; Stewart, M.; Ford, J.; O'Hair, R. A.; Williams, L.; Lacey, E.; Gill, J. H.; Heiland, K.; Friedel, T. *Org. Biomol. Chem.* **2003**, *1*, 1856.
(6) Kogen, H.; Kiho, T.; Nakayama, M.; Furukawa, Y.; Kinoshita, T.; Inukai, M. *J. Am. Chem. Soc.* **2000**, *122*, 10214.
(7) Song, Y.; Li, Q.; Liu, X.; Chen, Y.; Zhang, Y.; Sun, A.; Zhang, W.; Zhang, J.; Ju, J. *J. Nat. Prod.* **2014**, *77*, 1937.
(8) Zhou, X.; Huang, H.; Li, J.; Song, Y.; Jiang, R.; Liu, J.; Zhang, S.; Hua, Y.; Ju, J. *Tetrahedron* **2014**, *70*, 7795.
(9) Vaillancourt, F. H.; Yeh, E.; Vosburg, D. A.; O'Connor, S. E.; Walsh, C. T. *Nature* **2005**, *436*, 1191.
(10) Schadewaldt, P.; Bodner-Leidecker, A.; Hammen, H. W.; Wendel, U. *Pediatr. Res.* **2000**, *47*, 271.
(11) Schwarz, E. L.; Roberts, W. L.; Pasquali, M. *Clin. Chim. Acta* **2005**, *354*, 83.
(12) Sowell, J.; Pollard, L.; Wood, T. *J. Sep. Sci.* **2011**, *34*, 631.
(13) Strauss, K. A.; Puffenberger, E. G.; Morton, D. H. Maple Syrup Urine Disease. In *GeneReviews*; Pagon, R. A., Adam, M. P., Ardinger, H. H., Bird, T. D., Dolan, C. R., Fong, C. T., Smith, R. J. H., Stephens, K., Eds; University of Washington: Seattle, 2006; pp 71−88 [updated 2013 May 09].
(14) Wendel, U.; Langenbeck, U.; Seakins, J. W. *Pediatr. Res.* **1989**, *25*, 11.
(15) Schadewaldt, P.; Wendel, U. *Pediatr. Res.* **1987**, *22*, 591.
(16) Schadewaldt, P.; Wendel, U. *Biochem. Med. Metab. Biol.* **1989**, *41*, 105.
(17) Schadewaldt, P.; Bodner-Leidecker, A.; Hammen, H. W.; Wendel, U. *Clin. Chem.* **1999**, *45*, 1734.
(18) Li, Q.; Song, X.; Qin, X.; Zhang, X.; Sun, A.; Ju, J. *J. Nat. Prod.* **2015**, *78*, 944.
(19) Liu, J.; Wang, B.; Li, H.; Xie, Y.; Li, Q.; Qin, X.; Zhang, X.; Ju, J. *Org. Lett.* **2015**, *17*, 1509.
(20) Chen, C. D.; Lin, C. H.; Chuankhayan, P.; Huang, Y. C.; Hsieh, Y. C.; Huang, T. F.; Guan, H. H.; Liu, M. Y.; Chang, W. C.; Chen, C. J. *J. Bacteriol.* **2012**, *194*, 6206.
(21) Okada, K.; Hirotsu, K.; Sato, M.; Hayashi, H.; Kagamiyama, H. *J. Biochem.* **1997**, *121*, 637.
(22) Castell, A.; Mille, C.; Unge, T. *Acta Crystallogr., Sect. D: Biol. Crystallogr.* **2010**, *66*, 549.
(23) Yennawar, N. H.; Islam, M. M.; Conway, M.; Wallin, R.; Hutson, S. M. *J. Biol. Chem.* **2006**, *281*, 39660.
(24) Soding, J.; Biegert, A.; Lupas, A. N. *Nucleic Acids Res.* **2005**, *33*, W244.
(25) Ha, N. C.; Choi, G.; Choi, K. Y.; Oh, B. H. *Curr. Opin. Struct. Biol.* **2001**, *11*, 674.
(26) Gust, B.; Challis, G. L.; Fowler, K.; Kieser, T.; Chater, K. F. *Proc. Natl. Acad. Sci. U. S. A.* **2003**, *100*, 1541.
(27) Haruyama, K.; Nakai, T.; Miyahara, I.; Hirotsu, K.; Mizuguchi, H.; Hayashi, H.; Kagamiyama, H. *Biochemistry* **2001**, *40*, 4633.
(28) Zhang, Y.; Huang, H.; Chen, Q.; Luo, M.; Sun, A.; Song, Y.; Ma, J.; Ju, J. *Org. Lett.* **2013**, *15*, 3254.
(29) Gui, C.; Li, Q.; Mo, X.; Qin, X.; Ma, J.; Ju, J. *Org. Lett.* **2015**, *17*, 628.

DOI: 10.1021/jacs.5b11380
J. Am. Chem. Soc. 2016, 138, 408−415